

Weakly Supervised Person Search with Region Siamese Networks

Chuchu Han^{1*}, Kai Su², Dongdong Yu², Zehuan Yuan², Changxin Gao¹,
Nong Sang^{1,†}, Yi Yang³, Changhu Wang²

¹Key Laboratory of Ministry of Education for Image Processing and Intelligent Control,
School of Artificial Intelligence and Automation, Huazhong University of Science and Technology

²ByteDance ³University of Technology Sydney

{hcc, cgao, nsang}@hust.edu.cn Yi.Yang@uts.edu.au

{sukai, yudongdong, yuanzehuan, wangchanghu}@bytedance.com

Abstract

Supervised learning is dominant in person search, but it requires elaborate labeling of bounding boxes and identities. Large-scale labeled training data is often difficult to collect, especially for person identities. A natural question is whether a good person search model can be trained without the need of identity supervision. In this paper, we present a weakly supervised setting where only bounding box annotations are available. Based on this new setting, we provide an effective baseline model termed Region Siamese Networks (R-SiamNets). Towards learning useful representations for recognition in the absence of identity labels, we supervise the R-SiamNet with instance-level consistency loss and cluster-level contrastive loss. For instance-level consistency learning, the R-SiamNet is constrained to extract consistent features from each person region with or without out-of-region context. For cluster-level contrastive learning, we enforce the aggregation of closest instances and the separation of dissimilar ones in feature space. Extensive experiments validate the utility of our weakly supervised method. Our model achieves the rank-1 of 87.1% and mAP of 86.0% on CUHK-SYSU benchmark, which surpasses several fully supervised methods, such as OIM [36] and MGTS [4], by a clear margin. More promising performance can be reached by incorporating extra training data. We hope this work could encourage the future research in this field.

1. Introduction

Person search [36] aims to localize and recognize a query person from a gallery of unconstrained scene images. Despite tremendous progress achieved by recent works [36, 35, 26, 37, 11, 10, 5, 44], the training process

*This work was done when Chuchu Han was an intern at ByteDance.

†Corresponding author

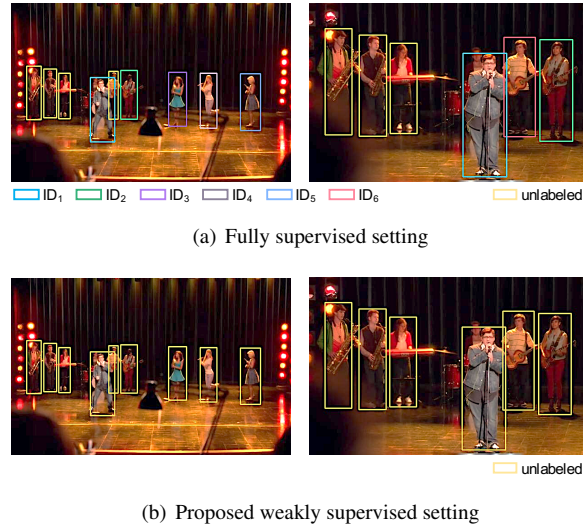


Figure 1. Comparisons between two settings. (a) Fully supervised setting. The images are annotated with both bounding boxes and person identities. Note that some identity annotations have lacked in original person search datasets. (b) The proposed weakly supervised setting. The images only have bounding box annotations.

requires strong supervision in terms of bounding boxes and identity labels, shown in Fig. 1(a). However, obtaining such annotations at a large scale can be time-consuming and economically expensive. Even in the most widely used dataset, CUHK-SYSU [36], almost 72.7% of pedestrian bounding boxes have no identity annotations. It indicates that labeling identities is more difficult than bounding boxes. The infeasible identity annotations largely restrict the scalability of supervised methods.

Instead of relying on the expensive labeling, a lot of researchers have been dedicated to training models with no labels [17, 7] or incomplete labels [27, 45] in the areas of image recognition, object detection, *etc.* Nevertheless, relevant explorations are missing in the field of person search. To fill the gap, we investigate the person search modeling in

a weakly supervised setting, where only bounding box annotations are required. As shown in Fig. 1(b), the proposed setting alleviates the burden of obtaining manually labeled identities. However, it is more challenging to pursue accurate person search using sole bounding box annotations.

In this paper, we setup a strong weakly supervised baseline called Region Siamese Networks (R-SiamNets). Towards learning meaningful feature representations of each instance, our model minimizes the discrepancy between two encoded features transformed from the same pedestrian region. Specifically, one branch is fed with the whole scene image and extracts the RoI features of the person instance. The other branch extracts features from the cropped person image. The obtained features from the two weight-sharing branches are constrained to be consistent. The motivation of this design is that the context-free instance features extracted from the cropped image regions could help the network to distinguish persons from the irrelevant background content. We formulate a self-instance consistency loss and an inter-instance similarity consistency loss to supervise the learning of context-invariant feature representations.

Further, a cluster-level contrastive learning method is introduced for striking a balance between separation and clustering. The clustering method aggregates the closest instances together and pushes instances from different clusters apart. It is assumed that the closest features have a high probability of being from the same individual. The generated pseudo labels by clustering are used for contrastive learning. We iteratively apply this non-parametric clustering for refinement along with the training process. The cluster-level contrastive learning yields a significant performance gain, with the 6.1% absolute improvement of mAP on the CUHK-SYSU dataset.

Our contributions can be summarized in three-folds:

- We introduce a weakly-supervised setting for person search. The new setting only requires bounding box annotations, relieving the burden of obtaining manually labeled identities. With this setting, the developed algorithms could be readily utilized for large-scale person search in real-world scenarios.
- We propose the R-SiamNet as a baseline under the weakly supervised setting. With the Siamese network, instance-level consistency learning is applied to encourage context-invariant representations. Further, cluster-level contrastive learning is introduced for striking a balance between separation and clustering.
- Our R-SiamNet achieves the rank-1 of 87.1% and 75.2% on CUHK-SYSU and PRW datasets, respectively. The results outperform several supervised methods by a clear margin, *e.g.*, OIM [36] and MGTS [4]. More promisingly, the performance is further promoted when incorporating more extra datasets.

2. Related Work

Person Search. Recently, person search task has raised a lot of interest in the computer vision community [36, 43, 4, 3, 21, 5, 42]. In the literature, there are two manners to deal with this problem, *i.e.*, two-step and one-step.

For two-step methods, the pedestrian detection and person re-identification are trained with two separated models [43, 4, 3, 21, 15]. Zheng *et al.* [43] evaluate various combinations of different detectors and re-ID networks, and develop a Confidence Weighted Similarity (CWS) to assist the pedestrian matching. Chen *et al.* [4] enhance the feature representations by introducing a mask-guided two-stream model. Han *et al.* [15] develop an RoI transform layer to optimize the two networks end-to-end. With more parameters, these methods guarantee high performance while low efficiency in evaluation.

One-step methods [36, 35, 16, 5] jointly train the detection and re-ID in a unified model, exhibiting high efficiency. Among these methods, [36, 35] take the Faster R-CNN [28] as a backbone network, and most layers are shared by two tasks. Munjal *et al.* [26] first introduce a query-guided end-to-end person search network. With the global context from both query and gallery images, the well-designed framework generates query-relevant proposals and learns query-guided re-ID scores. Yan *et al.* [37] explore the contextual information and build a graph learning framework to employ context pairs to update target similarity. Dong *et al.* [10] develop a bi-directional interaction network and employ the cropped person patches as the guidance to reduce redundant context influences.

These studies are fully supervised and require precise annotations for each person, including the bounding boxes and the identities. It is impractical to extend these methods in large-scale scenarios due to the expensive labeling process. Thus, we introduce a weakly supervised setting and develop a framework trained solely with bounding boxes.

Siamese Networks. Siamese networks [2] consist of twin networks which accept distinct inputs, and the comparability is determined by supervision. This architecture is widely used in many fields, including object tracking [1], one-shot learning [20], signature [2] and face verification [31], *etc.* In this paper, we explore the context-invariant embeddings based on a region Siamese network with two forms of inputs, *i.e.*, whole scene images, and cropped images.

Contrastive Learning. Contrastive learning [14] aims at attracting the positive sample pairs and repulsing the negative ones, which has been popularized in recent unsupervised learning [19, 34, 39, 17, 7, 8]. Wu *et al.* [34] consider each instance as a class, and employ a memory bank to store the instance embeddings. Similar to [34], Ye *et al.* [39] learn the data augmentation invariant and instance spread-

out features. MoCo [17] maintains the dictionary with a queue and a moving-averaged encoder, so the contrastive learning is viewed as the dictionary look-up. SimCLR [7] deprecates the usage of the memory bank, and directly uses negative samples in the current batch. In this paper, rather than only independently penalizing the incompatibility of each single positive pair at a time, we construct more informative positive pairs by non-parametric clustering.

Unsupervised Person Re-identification. The traditional unsupervised methods can be summarized into three categories, designing hand-craft features, utilizing localized saliency statistics, or dictionary learning-based works. However, the performance of these methods is inferior to supervised ones. On the basis of clustering algorithms, recent works exhibit higher performance. Lin *et al.* [24] develop a bottom-up clustering framework to iteratively train the network with pseudo labels. Zeng *et al.* [40] combine the hierarchical clustering method with hard-batch triplet loss. Ge *et al.* [13] design a self-paced contrastive learning strategy with a novel clustering reliability criterion to filter the unstable clusters with DBSCAN [12]. Although the cluster-based methods achieve high performance, they require carefully adjusted hyperparameters, *e.g.*, number of clusters [24, 40], or the distance threshold [12].

In this paper, we employ a non-parametric clustering method [29], with a filtering mechanism by image information. This manner only relies on the first neighbor of each data point, and requires no hyper-parameters.

3. Proposed Method

In this section, we first introduce the overall region Siamese network in Sec. 3.1. Then we will describe the instance-level consistency learning in Sec. 3.2. At last, the cluster-level contrastive learning is developed in Sec. 3.3.

3.1. Region Siamese Network

Our main target is to locate the person positions and learn representative features for identification. Under the weakly supervised setting, only the bounding box annotations are employed in the training process. Without manually labeled identities, it is essential to design supervision signals for training the network. To achieve this goal, we develop the framework from two aspects: 1) Based on Siamese networks, the comparability is determined by supervision with different augmented inputs. In this paper, both whole scene images and cropped images are taken as inputs. We focus on the instance-level consistency learning to encourage context-invariant embeddings. 2) Pseudo labels generated by clustering permit to model cluster-level supervision. Thus, we apply the cluster-level contrastive learning, reaching a balance between separation and aggregation.

Based on these considerations, we propose a region

Siamese network as shown in Fig. 2. There are two branches termed as search path and instance path. With an extra detection head, the search path takes the whole scene images as inputs, training the detection and identification jointly. The feature embedding of each pedestrian is generated by the Region-of-Interest (RoI) align layer. For the instance path, the cropped images are taken as inputs. With less context, the corresponding outputs can focus on the regions of pedestrians. To ensure the context-invariant embeddings, we apply the instance-level consistency learning on the output of two paths. It consists of a self-instance consistency loss and an inter-instance similarity consistency loss. Besides, to model the cluster-level supervision, we employ a non-parametric clustering method based on the nearest neighbor of each sample. A cluster-level contrastive loss is developed to calculate the similarities between the samples in the current batch and the memory bank. During inference, we only utilize the search path.

3.2. Instance-Level Consistency Learning

With no identity annotations, it is observed that the learned instance features are involved with excessive context. As a fine-grained task, the retrieval process is easily affected by interference from surrounding persons and noises. To alleviate this issue, we input the cropped pedestrians which contain less context to build the supervision. The instance-level consistency learning is developed to encourage the context-invariant embeddings from two aspects.

Self-instance consistency loss. Given a mini-batch of scene images, we obtain B cropped pedestrian images with bounding box labels. The scene images and cropped ones are processed by the region Siamese network. The output embeddings are denoted as $\mathbf{F}_a = [f_1^a, f_2^a, \dots, f_B^a]^T$ and $\mathbf{F}_b = [f_1^b, f_2^b, \dots, f_B^b]^T$ for search path and instance path, respectively. To encourage the context-invariant embeddings for a specific instance, we consider to maximize the cosine similarity between f^a and f^b . Then the self-instance consistency loss is defined as:

$$L_{ins} = \frac{1}{B} \sum_{i=1}^B \left(1 - \frac{f_i^a}{\|f_i^a\|_2} \cdot \frac{f_i^b}{\|f_i^b\|_2} \right), \quad (1)$$

where $\|\cdot\|_2$ is the L2 norm, and the loss is averaged over all instances in a mini-batch.

Inter-instance similarity consistency loss. The feature embeddings in each path can be seen as an aggregated feature space. The above self-instance consistency loss only constrains the embedding pairs from the same person to be closer individually. We further apply a constraint to enlarge the similarity distribution between the entire feature spaces. For the search path, the similarity matrix $\mathbf{S}^a \in \mathbb{R}^{B \times B}$ is obtained by $\mathbf{S}^a = \bar{\mathbf{F}}_a \bar{\mathbf{F}}_a^T$, where $\bar{\mathbf{F}}_a$ is produced by a row-wise L2 normalization on \mathbf{F}_a . In the same way, $\mathbf{S}^b \in \mathbb{R}^{B \times B}$

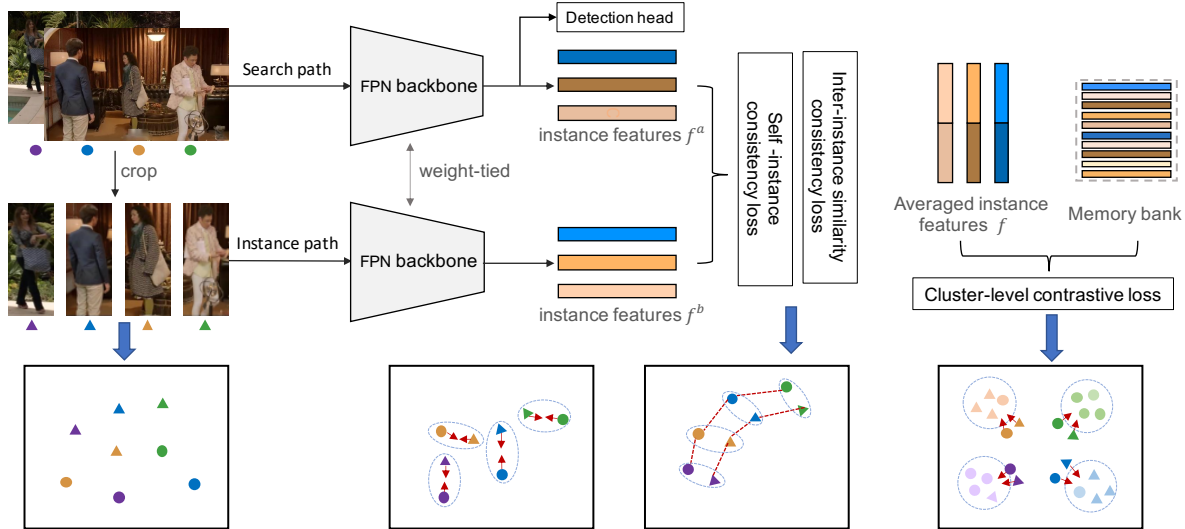


Figure 2. Illustration of our R-SiamNet for weakly supervised person search. Given whole scene images, the detection and identification are trained jointly with the backbone in the search path. The features of pedestrians are produced by the RoI align layer, denoted as f^a . Meanwhile, we introduce an instance path with the cropped persons as inputs. In this path, we extract the features f^b through the same layers. To encourage the context-invariant features, a self-instance consistency loss and an inter-instance similarity consistency loss are applied between f^a and f^b . Besides, pseudo labels are produced with the non-parametric clustering. We calculate the cluster-level contrastive loss between the averaged features f and the embeddings in memory bank. Note that only the search path is utilized in testing.

is calculated for the instance path. Our goal is to keep the consistency between the two similarity distributions. Based on the divergence, we develop an inter-instance similarity consistency loss as follows:

$$L_{int} = D_{KL}(\mathbf{S}^a || \mathbf{S}^b) + D_{KL}(\mathbf{S}^b || \mathbf{S}^a), \quad (2)$$

where D_{KL} denotes the KL divergence. It can be formulated as $D_{KL}(P||Q) = \sum_{x \in \mathbb{X}} P(x) \log(P(x)/Q(x))$. Since each distribution can be considered as the target, we adopt the mutual manner.

3.3. Cluster-Level Contrastive Learning

The instance recognition [34] treats each sample as a category to produce well-separated samples. In person search task, this approach may be inferior. We aim at exploring the similarities among persons and striking a balance between separation and aggregation. A non-parametric clustering method is employed to produce pseudo labels, and a cluster-level contrastive loss is applied between samples in the current batch and the memory bank.

Non-parametric clustering. We build the cluster-level supervision based on an assumption that the most similar feature embeddings have high probabilities of belonging to the same class. This motivates our clustering manner, in which only the nearest neighbor of each sample is aggregated. Meanwhile, there is a prior that the pedestrians in same scene images belong to different identities. Thus, we

can filter some false aggregations when clustering. After clustering, all persons are assigned pseudo labels.

Specifically, at the beginning of each epoch, the clustering process is conducted after extracting the embeddings of all instances. Supposing there are N samples, an adjacency matrix $\mathbf{A}(i, j) \in \mathbb{R}^{N \times N}$ can be constructed among all samples, which is initialized with all zeros. To set $\mathbf{A}(i, j) = 1$, two conditions should be satisfied simultaneously:

1) $j = \kappa_i^1$ or $\kappa_j^1 = i$ or $\kappa_i^1 = \kappa_j^1$, where κ_i^1 denotes the first neighbor of sample i . Besides the nearest neighbors, the adjacency matrix also links points that have the same neighbor with $\kappa_i^1 = \kappa_j^1$.

2) The whole scene image of the i -th and j -th pedestrian should be different. If two persons come from the same scene image, they cannot be clustered.

Different from other clustering algorithms that require carefully adjusted hyperparameters [24, 13, 40], e.g., cluster numbers or distance threshold, we employ the non-parametric clustering approach. It is easily scalable to large-scale data with minimal computational expenses.

Cluster-level contrastive loss. Similar to previous works [36, 5], we maintain a memory bank $\mathbf{M} \in \mathbb{R}^{N \times d}$ to store the embeddings of all instances, where d denotes the feature dimensions. After clustering, the memory bank is updated by the newly embedded features with pseudo labels. Then, a cluster-level contrastive loss can be computed between the features in the memory bank and current batch.

In a mini-batch, a specific instance feature is denoted as

Algorithm 1: Training procedure of R-SiamNet

Input : Unlabeled data $\mathbf{I} = \{I_1, I_2, \dots, I_{N'}\}$;
Scale factor γ ; Momentum λ
Initialization: Initialize the backbone with
ImageNet-pretrained ResNet-50.
for each epoch do
 1: Extract all the instance features.
 2: Conduct the non-parametric clustering.
 3: Update the features in the memory bank.
 for each mini-batch do
 1: Encode instance features of two paths through
 R-SiamNet:
 $f^a = \Phi_\theta(\mathbf{I})$
 $f^b = \Phi_\theta(\text{crop}(\mathbf{I}))$
 $f = \text{mean}(f^a, f^b)$
 2: Compute the self-instance consistency loss
 with Eq.1
 3: Compute the inter-instance similarity
 consistency loss with Eq. 2
 4: Compute the cluster-level contrastive loss with
 Eq.3
 5: During backward, update the features in
 memory bank:
 $M_t \leftarrow \lambda M_t + (1 - \lambda)f$
 end
end

$f = \text{mean}(f^a, f^b)$. Assuming that there are K positive samples in the memory bank sharing the same pseudo label with f . Then, the remaining J samples in \mathbf{M} are considered as negative samples. The cosine similarities are denoted as $\{s_p^i\}(i = 1, 2, \dots, K)$ and $\{s_n^j\}(j = 1, 2, \dots, J)$, respectively. Inspired by [30], we apply the cluster-level contrastive loss to make each s_p^i greater than s_n^j :

$$L_{clu} = \log[1 + \sum_{i=1}^K \sum_{j=1}^J \exp(\gamma(s_n^j - s_p^i))], \quad (3)$$

where γ is the scale factor. During backward, the memory bank is updated with the samples in current mini-batch: $M_t \leftarrow \lambda M_t + (1 - \lambda)f$. λ is the momentum factor and t denotes the instance position in the memory bank.

3.4. Training Procedure

Given the input images, we aim to learn a deep convolutional neural network (CNN) model Φ_θ to realize precise localization and identification. The details of our training procedure are provided in Algorithm 1. In summary, our total training objective is revised as:

$$L = L_{ins} + L_{int} + L_{clu} + L_{det}, \quad (4)$$

where L_{det} denotes the detection losses, including regression loss and foreground-background classification loss.

4. Experiments

In this section, we first introduce two benchmark datasets, followed by the settings under weakly supervised manner and evaluation protocols in Sec. 4.1. Then Sec. 4.2 describes the implementation details and the reproducibility. We conduct a series of ablation studies to analyze the effectiveness of the proposed method in Sec. 4.3. Finally, we discuss the comparison with the state of the arts in Sec. 4.4.

4.1. Datasets and Settings

CUHK-SYSU dataset. CUHK-SYSU [36] is a large-scale person search dataset, which is composed of urban scene pictures and movie snapshots. There are 18,184 images with 96,143 annotated bounding boxes, including 8,432 labeled identities. The training set consists of 11,206 images with 5,532 identities and several unlabeled ones. There are 6,978 gallery images and 2,900 probe images in testing set.

PRW dataset. PRW [43] is captured by six spatially disjoint cameras in the university. It consists of 11,816 frames with 43,110 annotated bounding boxes, among which 34,304 are assigned with 932 identity labels, and the rest are unlabeled ones. The training set contains 5,704 frames with 482 identities, and the testing set includes 6,112 gallery images and 2,057 queries with 450 identities.

Settings. Under the fully supervised setting, the statistics of the training data are shown in Tab. 1. In this paper, we propose a weakly supervised setting for person search, reducing the need of strong supervision during training. Under the weakly supervised setting, our model is trained only using 55,260 and 18,048 bounding box annotations for the CUHK-SYSU and PRW datasets, respectively.

Evaluation protocols. Our experiments employ the standard evaluation metrics in person search [36]. One is the cumulative matching cure (CMC), which is inherited from the person re-ID. A candidate is counted if the intersection-over-union (IoU) with ground truth is greater than 0.5. The other is the mean Average Precision (mAP), and it is inspired by the object detection task. For each query, we compute an averaged precision (AP) based on the precision-recall curve. Then, the mAP is calculated by averaging the APs across all the queries.

Table 1. Training data statistics on the CUHK-SYSU and PRW datasets within the fully supervised settings. Bbox: Bounding box.

Dataset	Images	IDs	Bboxes	
			Labeled	Unlabeled
CUHK-SYSU	11206	5532	15080 (27.3%)	40180 (72.7%)
PRW	5704	482	14906 (82.6%)	3142 (17.4%)

4.2. Implementation Details

Model. We employ RepPoints [38] released by OpenMMLab [6] as our backbone network, containing the ImageNet pretrained ResNet-50 [18], the feature pyramid network (FPN) [22], and a detection head. The search path takes the scene images as inputs, jointly training the detection and recognition. To obtain the pedestrian features f^a , the RoI align is applied on FPN with the ground truth RoIs, followed by a fully connected (fc) layer after flattening. For the instance path, the cropped and resized images are taken as inputs. Similar to f^a , f^b is produced with the same network except the RoI align, and both features are 2048-d.

Training. The scene images are resized to 1333×800 , and cropped images are rescaled to 192×64 . The batched Stochastic Gradient Descent (SGD) optimizer is used with a momentum of 0.9. The weight decay factor for L2 regularization is set to 5×10^{-4} . We use a mini-batch size of 9, and an initial learning rate of 1×10^{-3} . The model is trained for 48 epochs with the learning rate multiplied by 0.1 at 32 and 44 epochs. The scale factor γ is set to 16 and the momentum λ is set to 0.2 for both datasets. All experiments are implemented on the PyTorch framework, and the network is trained on the NVIDIA Tesla V100.

4.3. Ablation Study

To evaluate the effectiveness of the proposed framework, we conduct detailed ablation studies on the CUHK-SYSU and PRW datasets. Note that all the settings in each experiment are the same as the implementation in Sec. 4.2.

Effectiveness of different components. To verify the effectiveness of each component, we compare the performance under different settings in the training process. The results are shown in Tab. 2.

Instance Recognition (IR) [34] denotes that each instance is treated as a category in training. A memory bank is maintained to store all the instance features, providing abundant negative samples to compute the contrastive loss. *Search path w/ IR* means the supervision of IR is only applied on the instance features produced by the search path. This approach can be viewed as the baseline of our method. With the scene images as input, instance features may contain excessive context to disturb the matching, thus the mAP only reaches 51.85%. *Instance path w/ IR* indicates the IR is applied on the features generated by the instance path, which takes the cropped persons as inputs. In the search path, only the detection head is trained within the same backbone. Under this setting, the result can reach 63.79% on mAP. Compared to the search path, the instance path contains less context, exhibiting higher performance.

R-SiamNet w/ L_{ins} takes both scene images and cropped pedestrian images as inputs, and the fused outputs are super-

vised by IR. To encourage the context-invariant feature embeddings, we apply the *self-instance consistency loss* L_{ins} between two paths. It maximizes the similarity of pairwise features from two paths. The mAP is promoted to 76.06%, surpassing 51.85% by a large margin. This verifies the importance of keeping consistency. For further restraint, we develop the *inter-instance similarity consistency loss* L_{int} , which is applied on the similarity distributions within the mini-batch of two paths. This further guarantees the context-invariant embeddings, and achieves a gain of 3.96% on rank-1. Moreover, to explore the cluster-level supervision, we implement the non-parametric clustering to produce pseudo labels. Thus, a *cluster-level contrastive loss* L_{clu} is employed for supervision instead of IR. From Tab. 2, we can see that the performance achieves 85.72% on mAP and 86.86% on rank-1. The results show the effectiveness of our framework.

Table 2. Component analysis of our method. IR: Instance recognition. The rank-1/5/10 accuracy (%) and mAP (%) are shown.

Method	CUHK-SYSU			
	mAP	R1	R5	R10
Search path w/ IR	51.85	59.69	67.31	69.03
Instance path w/ IR	63.79	65.55	82.21	86.83
R-SiamNet w/ L_{ins} & IR	76.06	78.21	90.28	92.90
R-SiamNet w/ L_{ins} & L_{int} & IR	79.62	82.17	91.69	94.03
R-SiamNet w/ L_{ins} & L_{int} & L_{clu}	85.72	86.86	95.24	96.86

Scalability with different scales of training data. Our framework is designed to learn discriminative identity embeddings under the weakly supervised setting. The scalability is essential for the methods when giving more training data without identity labeling. To discuss the scalability, we design the experiment from two aspects.

First, we assess the performance with different percentages of training data individually, as shown above the dotted line in Tab. 3. Specifically, we divide the CUHK-SYSU/PRW dataset by 20%, 40%, 60%, 80%, 100% for training. It can be seen that the performance is gradually improved as the training scale increases. Moreover, the growing tendency has not reached saturation on both datasets, indicating that the proposed framework can achieve further improvement with more training data.

Second, to further evaluate the scalability of our method, we expand the training set by combining different datasets. The results are shown below the dotted line in Tab. 3. When training with CUHK-SYSU and PRW datasets together, the performance on both datasets has been considerably improved. Especially for the PRW dataset, the mAP is promoted by a large margin since the added CUHK-SYSU owns a larger data scale. Besides, we also employ a dataset called INRIA [9] in the pedestrian detection task. There are 902 images that contain 1,826 pedestrians with

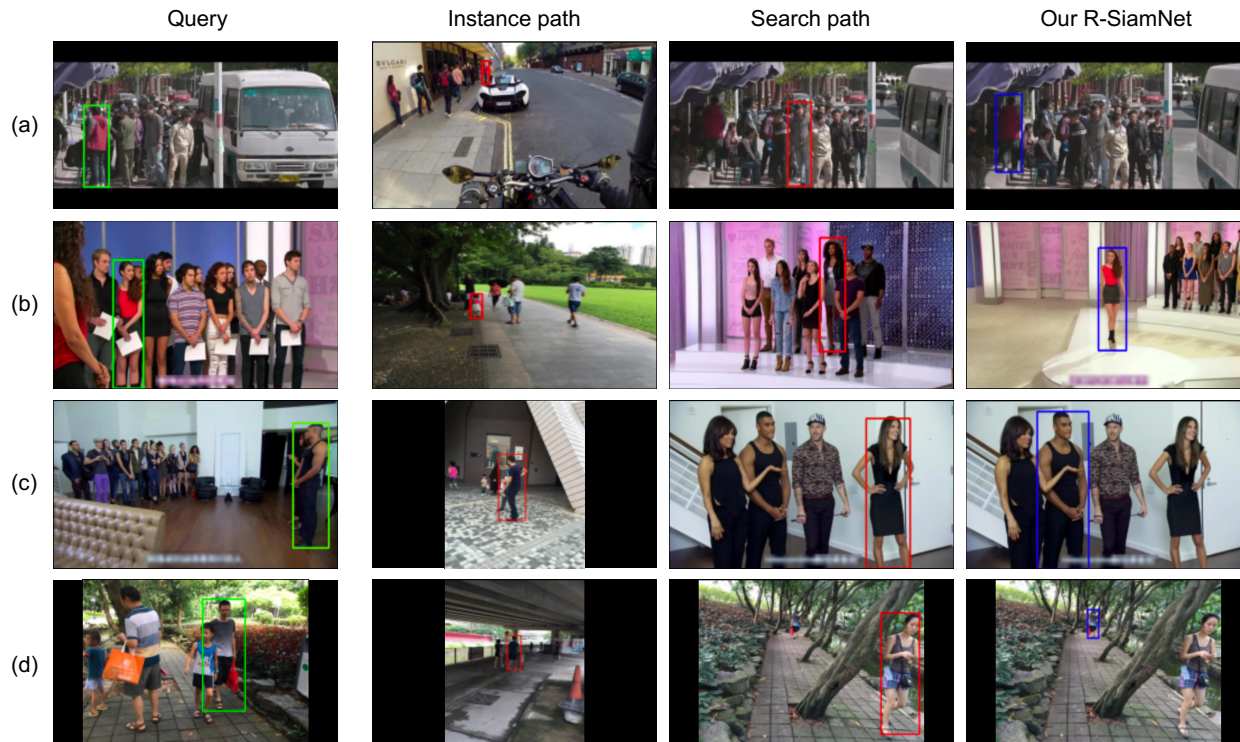


Figure 3. Visualization of different methods on the CUHK-SYSU dataset. Given the query images, we show the rank-1 search results of three training approaches. First column shows the query persons with the green boxes. The instance path/search path denote the model is trained with a single path. The last column show the result of our region Siamese network. Red/blue boxes represent the wrong/correct results, respectively.

bounding boxes labeling. When training with the three datasets together, our performance is further promoted on both CUHK-SYSU and PRW datasets.

All the experiments prove that our framework has the potential to reach promising performance by incorporating more training data.

Table 3. Performance with different scales of training set. Above the dotted line, the results with different percentages of training data are shown. Below the dotted line, it exhibits the performance of combining with more training datasets.

Training set	CUHK-SYSU		PRW	
	R1	mAP	R1	mAP
20% data	78.34	76.71	66.94	15.61
40% data	82.41	80.50	69.32	17.59
60% data	83.45	82.52	71.80	19.10
80% data	85.41	84.15	72.73	19.64
100% data	86.86	85.72	73.36	21.16
--- CUHK-SYSU & PRW ---	87.00	85.92	75.06	23.50
CUHK-SYSU & PRW & INRIA	87.59	86.19	76.03	25.53

Visualization and Analysis. To evaluate the effectiveness of the proposed method, we illustrate some qualitative search results on the CHUK-SYSU dataset. As Fig. 3

shows, we present the comparisons on rank-1 of our R-SiamNet and the other two manners. Specifically, the first column shows the query persons with green bounding boxes. Instance path/search path represents that the model employs the cropped images/whole scene images as input within a single path. The last column is the result of our R-SiamNet. The search results are exhibited with different colors, *i.e.*, red boxes denote the wrong matches while the blue boxes show the correct ones.

There are several observations from the visualization. First, it is observed that the wrong matches in the search path are definitely different from the query, but with similar contexts. This verifies the existence of excessive contexts, which disturb the matching process by involving more surrounding persons/backgrounds. Second, we find that most false examples in the instance path have a similar appearance with the query. This indicates the features are hardly disturbed by the contexts. Third, our R-SiamNet promotes the complementarity of both paths, maintaining useful context to aid the person search. The results also show the effectiveness of our method, which can successfully localize and match the query person in most cases.

Table 4. Experimental comparisons with state-of-the-art methods on the CUHK-SYSU and PRW datasets.

Methods		CUHK-SYSU		PRW		
		R1	mAP	R1	mAP	
two-step	Fully supervised setting:					
	RCAA [3]	81.3	79.3	-	-	
	MGTS [4]	83.7	83.0	72.1	32.6	
	CLSA [21]	88.5	87.2	65.0	38.7	
	RDLR [15]	94.2	93.0	70.2	42.9	
	TCTS [33]	95.1	93.9	87.5	46.8	
one-step	OIM [36]	78.7	75.5	49.9	21.3	
	IAN [35]	80.1	76.3	61.9	23.0	
	NPSM [25]	81.2	77.9	53.1	24.2	
	CTXGraph [37]	86.5	84.1	73.6	33.4	
	DC-I-Net [41]	86.5	86.2	55.1	31.8	
	QEEPS [26]	89.1	88.9	76.7	37.1	
	NAE [5]	92.4	91.5	80.9	43.3	
	NAE+ [5]	92.9	92.1	81.1	44.0	
	DMRNet [16]	94.2	93.2	83.3	46.9	
	Weakly supervised setting:					
	Ours (1333*800)	86.9	85.7	73.4	21.2	
	Ours (1500*900)	87.1	86.0	75.2	21.4	

4.4. Comparisons with the State-of-the-arts

In this section, we compare our proposed framework with current state-of-the-art methods on person search in Tab. 4. The results of two-step methods [3, 4, 21, 15, 33] are shown in the upper block while the one-step methods [36, 35, 25, 37, 41, 26, 5] in the lower block.

Evaluation on CUHK-SYSU. The comparisons between our network and existing supervised methods on the CUHK-SYSU dataset are shown in Tab. 4. When the gallery size is set to 100, our proposed method reaches 85.7% on mAP and 86.9% on rank-1. The performance can outperform several supervised methods. Moreover, when using a larger resolution of 1500×900 , our results are further improved and reach 86.0% on mAP and 87.1% on rank-1.

To evaluate the performance consistency, we also compare with other competitive methods under varying gallery sizes of [50, 100, 500, 1000, 2000, 4000]. Fig. 4 shows the comparisons with both one-step and two-step methods. It can be seen that the performance of all methods decreases as the gallery size increases. This indicates it is challenging when more distracting people are involved in the identity matching process, which is close to real-world applications. Our method outperforms some supervised methods under different gallery sizes.

Evaluation on PRW. We also evaluate our method on the PRW dataset, as shown in Tab. 4. Following the setting in benchmark [43], the gallery contains all the 6, 112 testing

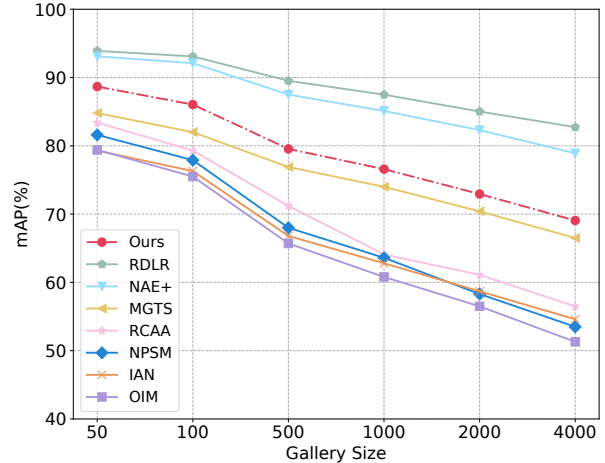


Figure 4. Comparisons with different gallery sizes on the CUHK-SYSU dataset. Our method is represented by dotted lines.

images. This is challenging since a tremendous number of detected bounding boxes are involved. Compared with the competitive techniques, our performance achieves 73.4% on rank-1, and it is further promoted with larger resolutions. Our method surpasses most works in both one-step and two-step manners. However, the results exhibit a low mAP due to the minor inter-class variations in this dataset.

5. Conclusion

In this paper, we introduce a weakly supervised setting for the person search task to alleviate the burden of costly labeling. Under this new setting, no specific identity annotations of pedestrians are required, and we only utilize the accessible bounding boxes for training. Meanwhile, we propose a baseline called R-SiamNet for localizing persons and learning discriminative feature representations. To encourage the context-invariant features, a self-instance consistency loss and an inter-instance similarity consistency loss are developed. We also explore the balance between separation and aggregation by a cluster-level contrastive loss. Extensive experimental results on the widely used benchmarks demonstrate the effectiveness of our framework. The results also show that the gap with supervised state-of-the-arts will be further narrowed with more training data.

Acknowledgements

This work was partially supported by the Project of the National Natural Science Foundation of China No. 61876210, the Fundamental Research Funds for the Central Universities No.2019kfyXKJC024, and the 111 Project on Computational Intelligence and Intelligent Control under Grant B18024.

References

- [1] Luca Bertinetto, Jack Valmadre, Joao F Henriques, Andrea Vedaldi, and Philip HS Torr. Fully-convolutional siamese networks for object tracking. In *European Conference on Computer Vision*, 2016.
- [2] Jane Bromley, Isabelle Guyon, Yann LeCun, Eduard Säckinger, and Roopak Shah. Signature verification using a” siamese” time delay neural network. *Advances in Neural Information Processing Systems*, 1994.
- [3] Xiaojun Chang, Po-Yao Huang, Yi-Dong Shen, Xiaodan Liang, Yi Yang, and Alexander G Hauptmann. Rcaa: Relational context-aware agents for person search. In *European Conference on Computer Vision*, 2018.
- [4] Di Chen, Shanshan Zhang, Wanli Ouyang, Jian Yang, and Ying Tai. Person search via a mask-guided two-stream cnn model. In *European Conference on Computer Vision*, 2018.
- [5] Di Chen, Shanshan Zhang, Jian Yang, and Bernt Schiele. Norm-aware embedding for efficient person search. In *IEEE Conference on Computer Vision and Pattern Recognition*, 2020.
- [6] Kai Chen, Jiaqi Wang, Jiangmiao Pang, Yuhang Cao, Yu Xiong, Xiaoxiao Li, Shuyang Sun, Wansen Feng, Ziwei Liu, Jiarui Xu, et al. MMDetection: Open mmlab detection toolbox and benchmark. *arXiv preprint arXiv:1906.07155*, 2019.
- [7] Ting Chen, Simon Kornblith, Mohammad Norouzi, and Geoffrey Hinton. A simple framework for contrastive learning of visual representations. In *International conference on machine learning*, 2020.
- [8] Xinlei Chen and Kaiming He. Exploring simple siamese representation learning. *arXiv preprint arXiv:2011.10566*, 2020.
- [9] Navneet Dalal and Bill Triggs. Histograms of oriented gradients for human detection. In *IEEE Conference on Computer Vision and Pattern Recognition*, 2005.
- [10] Wenkai Dong, Zhaoxiang Zhang, Chunfeng Song, and Tieniu Tan. Bi-directional interaction network for person search. In *IEEE Conference on Computer Vision and Pattern Recognition*, 2020.
- [11] Wenkai Dong, Zhaoxiang Zhang, Chunfeng Song, and Tieniu Tan. Instance guided proposal network for person search. In *IEEE Conference on Computer Vision and Pattern Recognition*, 2020.
- [12] Martin Ester, Hans-Peter Kriegel, Jörg Sander, Xiaowei Xu, et al. A density-based algorithm for discovering clusters in large spatial databases with noise. In *Kdd*, 1996.
- [13] Yixiao Ge, Dapeng Chen, Feng Zhu, Rui Zhao, and Hongsheng Li. Self-paced contrastive learning with hybrid memory for domain adaptive object re-id. *arXiv preprint arXiv:2006.02713*, 2020.
- [14] Raia Hadsell, Sumit Chopra, and Yann LeCun. Dimensionality reduction by learning an invariant mapping. In *IEEE Conference on Computer Vision and Pattern Recognition*, 2006.
- [15] Chuchu Han, Jiacheng Ye, Yunshan Zhong, Xin Tan, Chi Zhang, Changxin Gao, and Nong Sang. Re-id driven localization refinement for person search. In *IEEE International Conference on Computer Vision*, 2019.
- [16] Chuchu Han, Zhedong Zheng, Changxin Gao, Nong Sang, and Yi Yang. Decoupled and memory-reinforced networks: Towards effective feature learning for one-step person search. In *Proceedings of the AAAI Conference on Artificial Intelligence*, 2021.
- [17] Kaiming He, Haoqi Fan, Yuxin Wu, Saining Xie, and Ross Girshick. Momentum contrast for unsupervised visual representation learning. In *IEEE Conference on Computer Vision and Pattern Recognition*, 2020.
- [18] Kaiming He, Xiangyu Zhang, Shaoqing Ren, and Jian Sun. Deep residual learning for image recognition. In *IEEE Conference on Computer Vision and Pattern Recognition*, 2016.
- [19] R Devon Hjelm, Alex Fedorov, Samuel Lavoie-Marchildon, Karan Grewal, Phil Bachman, Adam Trischler, and Yoshua Bengio. Learning deep representations by mutual information estimation and maximization. In *International Conference on Learning Representations*, 2018.
- [20] Gregory Koch, Richard Zemel, and Ruslan Salakhutdinov. Siamese neural networks for one-shot image recognition. In *ICML deep learning workshop*, 2015.
- [21] Xu Lan, Xiatian Zhu, and Shaogang Gong. Person search by multi-scale matching. In *European Conference on Computer Vision*, 2018.
- [22] Tsung-Yi Lin, Piotr Dollár, Ross Girshick, Kaiming He, Bharath Hariharan, and Serge Belongie. Feature pyramid networks for object detection. In *IEEE Conference on Computer Vision and Pattern Recognition*, 2017.
- [23] Tsung-Yi Lin, Priya Goyal, Ross Girshick, Kaiming He, and Piotr Dollár. Focal loss for dense object detection. In *IEEE International Conference on Computer Vision*, 2017.
- [24] Yutian Lin, Xuanyi Dong, Liang Zheng, Yan Yan, and Yi Yang. A bottom-up clustering approach to unsupervised person re-identification. In *Proceedings of the AAAI Conference on Artificial Intelligence*, 2019.
- [25] Hao Liu, Jiashi Feng, Zequn Jie, Karlekar Jayashree, Bo Zhao, Meibin Qi, Jianguo Jiang, and Shuicheng Yan. Neural person search machines. In *IEEE International Conference on Computer Vision*, 2017.
- [26] Bharti Munjal, Sikandar Amin, Federico Tombari, and Fabio Galasso. Query-guided end-to-end person search. In *IEEE Conference on Computer Vision and Pattern Recognition*, 2019.
- [27] Maxime Oquab, Léon Bottou, Ivan Laptev, and Josef Sivic. Is object localization for free?-weakly-supervised learning with convolutional neural networks. In *IEEE Conference on Computer Vision and Pattern Recognition*, 2015.
- [28] Shaoqing Ren, Kaiming He, Ross Girshick, and Jian Sun. Faster r-cnn: Towards real-time object detection with region proposal networks. In *Advances in Neural Information Processing Systems*, 2015.
- [29] Saquib Sarfraz, Vivek Sharma, and Rainer Stiefelhagen. Efficient parameter-free clustering using first neighbor relations. In *IEEE Conference on Computer Vision and Pattern Recognition*, 2019.
- [30] Yifan Sun, Changmao Cheng, Yuhang Zhang, Chi Zhang, Liang Zheng, Zhongdao Wang, and Yichen Wei. Circle loss: A unified perspective of pair similarity optimization. In *IEEE*

Conference on Computer Vision and Pattern Recognition, 2020.

- [31] Yaniv Taigman, Ming Yang, Marc' Aurelio Ranzato, and Lior Wolf. Deepface: Closing the gap to human-level performance in face verification. In *IEEE Conference on Computer Vision and Pattern Recognition*, 2014.
- [32] Laurens Van der Maaten and Geoffrey Hinton. Visualizing data using t-sne. *Journal of Machine Learning Research*, 2008.
- [33] Cheng Wang, Bingpeng Ma, Hong Chang, Shiguang Shan, and Xilin Chen. Tcts: A task-consistent two-stage framework for person search. In *IEEE Conference on Computer Vision and Pattern Recognition*, 2020.
- [34] Zhirong Wu, Yuanjun Xiong, Stella X Yu, and Dahua Lin. Unsupervised feature learning via non-parametric instance discrimination. In *IEEE Conference on Computer Vision and Pattern Recognition*, 2018.
- [35] Jimin Xiao, Yanchun Xie, Tammam Tillo, Kaizhu Huang, Yunchao Wei, and Jiashi Feng. Ian: the individual aggregation network for person search. *Pattern Recognition*, 2019.
- [36] Tong Xiao, Shuang Li, Bochao Wang, Liang Lin, and Xiaogang Wang. Joint detection and identification feature learning for person search. In *IEEE Conference on Computer Vision and Pattern Recognition*, 2017.
- [37] Yichao Yan, Qiang Zhang, Bingbing Ni, Wendong Zhang, Minghao Xu, and Xiaokang Yang. Learning context graph for person search. In *IEEE Conference on Computer Vision and Pattern Recognition*, 2019.
- [38] Ze Yang, Shaohui Liu, Han Hu, Liwei Wang, and Stephen Lin. Reppoints: Point set representation for object detection. In *IEEE International Conference on Computer Vision*, 2019.
- [39] Mang Ye, Xu Zhang, Pong C Yuen, and Shih-Fu Chang. Unsupervised embedding learning via invariant and spreading instance feature. In *IEEE Conference on Computer Vision and Pattern Recognition*, 2019.
- [40] Kaiwei Zeng, Munan Ning, Yaohua Wang, and Yang Guo. Hierarchical clustering with hard-batch triplet loss for person re-identification. In *IEEE Conference on Computer Vision and Pattern Recognition*, 2020.
- [41] Lei Zhang, Zhenwei He, Yi Yang, Liang Wang, and X-B Gao. Tasks integrated networks: Joint detection and retrieval for image search. *IEEE Transactions on Pattern Analysis and Machine Intelligence*, 2020.
- [42] Xinyu Zhang, Xinlong Wang, Jia-Wang Bian, Chunhua Shen, and Mingyu You. Diverse knowledge distillation for end-to-end person search. In *Proceedings of the AAAI Conference on Artificial Intelligence*, 2021.
- [43] Liang Zheng, Hengheng Zhang, Shaoyan Sun, Manmohan Chandraker, Yi Yang, and Qi Tian. Person re-identification in the wild. In *IEEE Conference on Computer Vision and Pattern Recognition*, 2017.
- [44] Yingji Zhong, Xiaoyu Wang, and Shiliang Zhang. Robust partial matching for person search in the wild. In *IEEE Conference on Computer Vision and Pattern Recognition*, 2020.
- [45] Zhi-Hua Zhou. A brief introduction to weakly supervised learning. *National science review*, 2018.

A. Additional Experimental Results

A.1. Paths for Evaluation

In our paper, the instance path is only applied in training, facilitating the identity feature learning of the main search path. During inference, we drop the instance path and the images are only passed through the search path. We compare the results of using different paths for testing, as shown in Tab. 5. It can be seen that using two paths for evaluation cannot bring extra performance gains. This indicates the context-invariant embeddings produced by our framework.

Table 5. Comparisons of using different paths for evaluation on the CUHK-SYSU dataset.

Inference path	mAP	Rank-1
Two paths	85.65	86.73
Search path	85.72	86.86

A.2. Different Detection Networks

Following [16], we choose the RepPoints as the detection network. To show the expandability of our R-SiamNet, different detectors are incorporated into our framework, including Faster R-CNN [28], RetinaNet [23] and RepPoints [38]. As reported in Tab. 6, the final performance gaps among different detectors are small, exhibiting the effectiveness and robustness of our framework.

Table 6. Comparisons when incorporated with different detectors on the CUHK-SYSU dataset.

Detector	mAP	Rank-1
Faster R-CNN	84.84	85.72
RetinaNet	85.39	86.59
RepPoints	85.72	86.86

A.3. Comparisons with Two-Step Manner

We combine a well-trained RepPoints detector [38] and an unsupervised re-ID model called SPCL [13] as our two-step competitor. As shown in Tab. 7, our method outperforms it by a large margin with higher efficiency. It shows that training detection and identification end-to-end is beneficial for obtaining better representations. It may also imply the importance of instance-level consistency learning.

Table 7. Comparisons with two-step manner on the CUHK-SYSU dataset.

Methods	mAP	Rank-1
RepPoints+SPCL	73.43	74.79
Ours	85.72	86.86

A.4. Evaluation on filter strategy in the clustering.

To analyze the effectiveness of the filter strategy in clustering, we conduct experiments with/without filtering by image information. As shown in Tab. 8, we observe 1.22%/1.13% rank-1 drops on CUHK-SYSU/PRW datasets by removing the filter strategy. This shows that it is beneficial to filter the aggregation of the persons from the same scene images.

Table 8. Performance of our method with/without the filter strategy in clustering. Results on the CUHK-SYSU and PRW datasets are shown. R-SiamNet w/o filter means the clustering is applied without filtering by image information.

Methods	CUHK-SYSU		PRW	
	mAP	Rank-1	mAP	Rank-1
R-SiamNet w/o filter	84.74	85.64	20.31	72.23
R-SiamNet	85.72	86.86	21.16	73.36

A.5. Different numbers of training epochs

We illustrate the mAP scores with different numbers of training epochs. As Fig. 5 shows, the results of three data scales are exhibited on the CUHK-SYSU dataset. It can be observed that the performance improves steadily to saturation as the epoch increases. With smaller data scales, the mAP reaches saturation earlier.

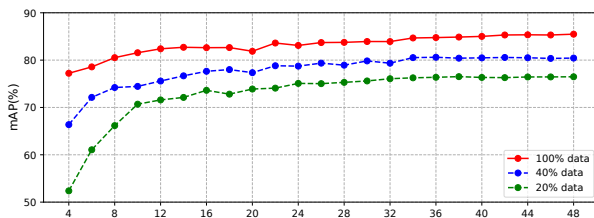


Figure 5. Performance with different numbers of training epochs. The results of three data scales are exhibited on the CUHK-SYSU dataset.

A.6. Runtime Comparisons

To compare the evaluation efficiency of our framework with other methods, we report the average runtime of the inference stage for a whole scene image, shown in Tab. 9. Since these methods are evaluated with different GPUs, we also exhibit the Tera-Floating Point Operation per-second (TFLOPs) for fair comparisons. Similar to other methods [5, 26, 4], we evaluate the models with an input image size of 900×1500 . As shown in Tab. 9, our R-SiamNet takes 72 milliseconds to process one image, which is faster than the two-step method MGTS [4] by a large margin. The query-guided method QEEPS [26] requires to re-compute

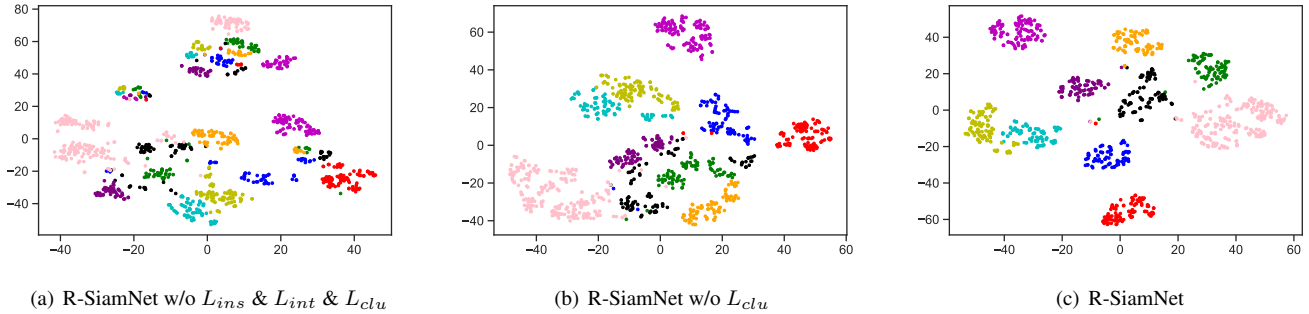


Figure 6. T-SNE feature visualization on a part of the PRW training set (10 classes, 1,089 pedestrians). (a) R-SiamNet without L_{ins} & L_{int} & L_{clu} . (b) R-SiamNet without L_{clu} . (c) Our proposed R-SiamNet with both instance-level consistency learning and cluster-level contrastive learning. Colors denote person identities.

all the gallery embeddings for each query image. This time-consuming operation reduces the evaluation efficiency. Moreover, our method is 13% faster than NAE [5]. These results clearly demonstrate the efficiency of our R-SiamNet in evaluation.

Table 9. Runtime comparisons of different methods when evaluation. The average runtime for one image with the size of 900×1500 is exhibited on the CUHK-SYSU dataset.

Methods	GPU (TFLOPs)	Runtime (ms)
MGTS [4]	K80 (8.7)	1269
QEEPS [26]	P6000 (12.0)	300
NAE+ [5]	V100 (14.1)	98
NAE [5]	V100 (14.1)	83
Ours	V100 (14.1)	72

the class are gathered loosely, and the margins among different classes are not clear. Furthermore, we apply the cluster-level contrastive learning, and the result is shown in Fig. 6(c). It can be seen that both intra-class compactness and inter-class separability are further encouraged. There are obvious margins among most categories. This verifies that our R-SiamNet can generate discriminative embeddings under the weakly supervised settings.

B. More Qualitative Analysis

B.1. Feature Visualization

To analyze the discriminative ability of our learned features, we employ the t-SNE [32] to visualize the feature representations in training. As illustrated in Fig. 6, there are 1,089 pedestrians with 10 classes, which is a subset of the PRW training set. Different colors represent different classes.

Fig. 6(a) shows the result when training with a single search path. Without applying the instance-level consistency learning and cluster-level contrastive learning, the learned features show large intra-class distances and small inter-class distances. When adding the instance-level consistency learning, including L_{ins} and L_{int} , the result is shown in Fig. 6(b). It is observed that the feature embeddings of the same category can be aggregated compared with Fig. 6(a). This shows the effectiveness of our instance-level consistency learning. Nevertheless, the features within